ChemComm

Accepted Manuscript

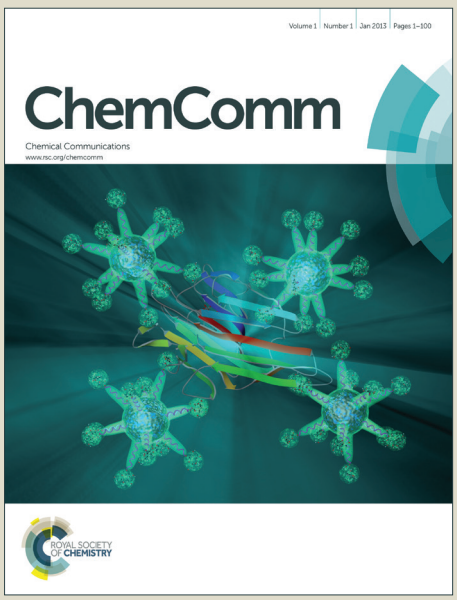

ROYAL SOCIETY OF CHEMISTRY

www.rsc.org/chemcomm

Chemical Communication ChemComm

Cite this: DOI: 10.1039/c0xx00000x

www.rsc.org/xxxxxx

COMMUNICATION

Polypyrrole hollow nanospheres: Stable cathode materials for sodium-ion batteries†

Dawei Su,*[,a] Jinqiang Zhang,[a] Shixue Dou[b] and Guoxiu Wang*[,a,c]

Received (in XXX, XXX) Xth XXXXXXXXX 20XX, Accepted Xth XXXXXXXXX 20XX
DOI: 10.1039/b000000x

Hollow polypyrrole (PPy) nanospheres with high sodium storage capacity as cathode materials for Na-ion batteries were reported. PPy hollow nanospheres demonstrated high current rate capacity and good cyclability. It was revealed by electrochemical testing and DFT calculation that the as-prepared PPy hollow nanospheres participate in reversible doping / de-doping reactions.

Na-ion batteries have attracted extensive interests for large-scale energy storage and conversion due to the low cost, abundant supply, and widespread terrestrial reserves of sodium mineral salts. Na-ion batteries also demonstrate similar features to lithium-ion batteries, including the use of non-aqueous electrolytes, alkali insertion electrodes.[1, 2] However, the higher ionization potential and larger ionic diameter of the Na ion ((1.02 Å) *vs.* Li (0.76 Å))[3] limit the structural variability and choice of crystalline sodium insertion materials. Therefore, finding and optimizing suitable electrode materials are crucial challenges for Na-ion batteries. Currently, the majority of studies have been focused on the development of appropriate active materials with sufficiently large interstitial space within their crystallographic structure to host sodium ions and achieve satisfactory electrochemical performance. These include layered oxides of the $NaMO_2$ (M = Co, Mn, or Ni) type,[4, 5] phosphate polyanion,[6, 7] sodium superionic conductor (NASICON)-type materials,[8] and sodium metal fluorophosphates.[9-11] Those electrode materials are limited by their crystal structures. More open tunnels for sodium ions insertion/extraction are the key factors for improving electrochemical performances.

Polymers have a flexible framework, which make them ideal candidates to accommodate larger Na ions reversibly without much spatial hindrance, facilitating fast kinetics for Na ions storage.[12-15] Moreover, redox-active polymers have diverse structures. They are also low-cost, environmentally friendly, and possibly accessible from abundant biomass resources. Therefore, redox-active polymers are promising electrode materials for Na-ion batteries.[16]

Recently, it was reported that there are feasible applications for nitro-substituted polyaniline[15] as cathode material and *n*-type polythiophene[17] as an anodic host for Na-ion batteries. One difficulty in developing polymer Na-storage electrodes is that the redox reactions suffer from a low level of sodium storage and slow kinetics, leading to poor capacity utilization of the polymer chains. [16]

Herein, we report the synthesis of polypyrrole (PPy) hollow nanospheres with high sodium storage capacity, using poly(methyl methacrylate) (PMMA) nanospheres as templates. The as-prepared PPy polymers were applied as cathode materials for Na ion batteries. Due to the improved sodium storage, the kinetics could be increased between the as-prepared PPy and the Na ion, enhancing utilization of the polymer chains. The PPy hollow nanospheres demonstrated high current rate capacity and cyclablity as cathodes in Na-ion batteries. Through characterizations by *ex-situ* scanning electron microscopy (SEM), transmission electron microscopy (TEM), Fourier transform infrared (FTIR) spectroscopy, and Raman spectroscopy, it was revealed that the redox reactions in the PPy cathodes take place through a doping / de-doping mechanism.

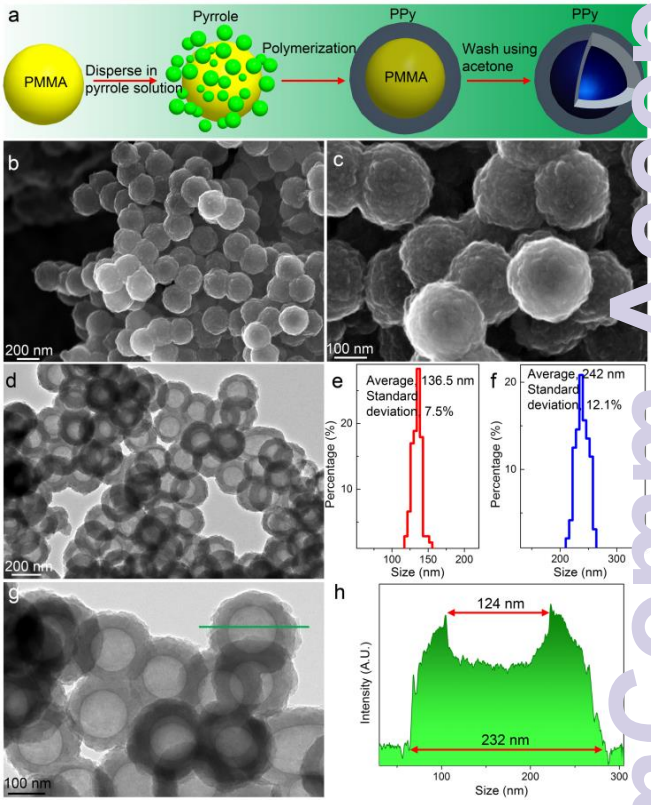

Fig. 1. (a) Schematic diagram of the synthesis of PPy hollow nanospheres. (b) Low and (c) high magnification field emission SEM (FESEM) images of as-prepared PPy hollow nanospheres. (d) TEM image of as-prepared PPy hollow nanospheres. Size distributions of the (e) inner and (f) outer diameters of the PPy hollow nanospheres. (g) High magnification TEM image of PPy hollow nanospheres. (h) Electron signal counts from the cross-section of the PPy hollow nanosphere marked in (g).

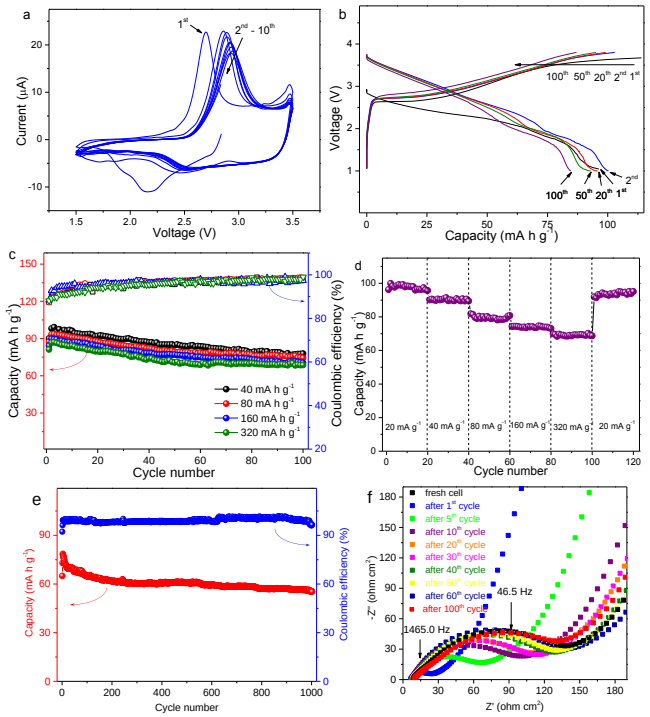

Fig. 2. (a) CV curves for the first 10 cycles of the PPy hollow nanosphere cathode for Na-ion batteries. (b) The 1st, 2nd, 20th, 50th, and 100th cycle discharge and charge profiles of the PPy hollow nanosphere cathode at current density of 20 mA g^{-1}. (c) Discharge capacity *vs.* cycle number at current densities of 40, 80, 160, and 320 mA g^{-1}. (d) The rate performance of the PPy hollow nanosphere cathode at varied current densities. (e) Long-term cycling performance and corresponding coulombic efficiency of PPy hollow nanospheres at current density of 400 mA g^{-1}. (f) Nyquist diagram of the PPy hollow nanospheres electrode before and after different charge and discharge cycles at 100 mA g^{-1} current density.

Fig. 1(a) is a schematic diagram which illustrates the synthesis of PPy hollow nanospheres. The PMMA nanospheres were first synthesized with a diameter of about 130 nm and a uniform size distribution (as shown in Fig. S1, Supporting Information, SI). After dispersing PMMA nanospheres in the distilled water, the pyrrole solution was added. Then, pyrrole monomers were polymerized in an ice bath using iron chloride as oxidant. After stirring for 3 h, the color of the solution changed to black, indicating the completion of the reaction. Finally, the PMMA was simply washed away with acetone. As shown in Fig. 1(b, c), the as-prepared PPy preserves the spherical shape of the templates with a homogeneous size distribution, without discernible shrinkage or structural deformation. From Fig. S2 (SI), it can be observed that the PPy nanospheres have a hollow structure. The change in contrast from the edge to the centre of each PPy sphere in the TEM images confirms that all spheres have a hollow architecture (Fig. 1(d, g)). To examine the uniformity of the synthesized PPy hollow nanospheres, we statistically analysed the values of the inner and outer diameters. The results are presented in Fig. 1(e) and (f), respectively. The average values of the inner and outer diameters are 136.5 nm and 242 nm with relative standard deviations of 7.5 % and 12.1 %, respectively. Each nanosphere features a shell about50 nm in thickness. The high magnification TEM image of PPy hollow nanospheres (Fig. 1(g)) confirms that the PMMA nanosphere templates were completely removed. Furthermore, the electron signal intensity measurement on the cross-section of the PPy nanosphere (Fig. 1(h)) shows that the inner part of the nanosphere presents fewer counts, which indicates the vacant inner space. Meanwhile, the electron signal intensity on the cross-section of the PPy hollow nanosphere demonstrates that there are no voids in the shells of the PPy hollow nanospheres. More TEM images of the as-prepared PPy hollow nanospheres are shown in Fig. S3 (SI). The specific Brunauer-Emmett-Teller (BET) surface area and Barrett-Joyner-Halenda (BJH) desorption pore volume were determined to be 34.01 m^2 g^{-1} and 0.14 cm^3 g^{-1}, respectively, which is deduced from the nitrogen sorption isotherm (Fig. S4 (SI)).

When the as-prepared PPy hollow nanospheres were used as cathodes for Na-ion storage in Na-ion batteries, the electrochemical reactions during the charge and discharge processes were first characterized by cyclic voltammetry, as shown in Fig. 2(a). We can observe the redox peaks at 2.16 V in the cathodic process and 2.7 V in the anodic process in the initial cycle. From the second cycle, a pair of well-defined redox peaks with almost the same peak areas appear at 2.5 and 2.8 V, indicating the reversible doping reaction of the PPy polymer.[13, 14] The *p*-type redox bands reflect the doping / de-doping reactions of ions into/from the polymer chains.[16] Furthermore, the peak areas are very similar after the second cycle and remain steady for the subsequent 10 cycles, suggesting high Coulombic efficiency and good cycling stability of the *p*-type redox reaction.

Accordingly, galvanostatic charge/discharge curves were collected at 20 mA g^{-1} for the PPy hollow nanospheres (Fig. 2(b)). The PPy nanospheres exhibit sloping charge and discharge curves. The PPy hollow nanospheres achieved reversible discharge capacity of 97 mA h g^{-1} in the first cycle. It should be noted that the PPy electrode delivered a higher discharge capacity of 100 mA h g^{-1} in the second cycle, corresponding the 4 unit PPy can absorbe 1 Na ion ($[C_4H_5N]_4Na$). Moreover, after 100 cycles, the as-prepared PPy hollow nanospheres still retain a discharge capacity of 85 mA h g^{-1}, suggesting their superior cyclability. The cyclability and rate capability of the PPy hollow nanospheres at different current densities are presented in Fig. 2(c). It can be seen that the PPy hollow nanosphere electrodes show satisfactory cycling performances at different current densities and a good high rate performance. The electrodes achieved high discharge capacities of 100, 94, 90, and 87 mA h g^{-1}, at the current densities of 40, 80, 160, and 320 mA g^{-1}, respectively. The as-prepared PPy hollow nanospheres show much better high rate performance than the $NaMO_2$ (M = Co, Mn, or Ni) type[18-21] and phosphate polyanion[6, 7] cathode materials for Na-ion batteries. After 100 cycles, the discharge capacities were maintained at high values: 74 mA h g^{-1} at 40 mA g^{-1}, 74 mA h g^{-1} at 80 mA g^{-1}, and 70 mA h g^{-1} at 160 mA g^{-1}. Even when cycled at 320 mA g^{-1}, 78 % discharge capacity (68 mA h g^{-1}) was maintained after 100 cycles. Furthermore, the PPy electrodes also presented high coulombic efficiencies at high current densities.

When cycled at varied high rates (Fig. 2(d)), the PPy hollow nanosphere cathode delivered a surprisingly high rate capability with reversible capacities of 100 mA h g^{-1} and 69 mA h g^{-1} at 20 mA g^{-1} and 320 mA g^{-1}, respectively. After cycling at high current densities, the cell capacity can recover to the original values when the current density is reversed back to the original low value, signifying their tolerance towards high rate cycling. To investigate the oxidization and cycling performance at high current densities of the as-prepared PPy hollow nanospheres, we conducted the long-term cycling test (up to 1000 cycles) at current density of 400 mA g^{-1} as shown in Fig. 2(e). It can be seen that at high current density, the as-prepared PPy hollow nanospheres still can achieve capacity of about 70 mA h g^{-1}. Furthermore, after 1000 charge and discharge cycles, it maintained 78.5 % of the capacity (~ 55 mA h g^{-1}) with high Coulombic efficiency, suggesting its good

cyclability at high current density and it is a promising material as a cathode in battery.

We also measured charge transfer resistance of the PPy hollow nanospheres electrode before and after different charge and discharge cycles to investigate the interface of polypyrrole/electrolyte as shown in Fig. 2(f) (the display in each of the Nyquist diagrams two frequencies in the region of low and intermediate frequencies can be seen in Fig. S5, SI). It can be seen that the fresh cell showed the charge transfer resistance of ~ 151 Ω cm^2, while after the initial discharge and charge processes, the charge transfer resistance decreased to the ~ 19 Ω cm^2. It consists with the galvanostatic charge/discharge testing result that after the first cycle, the capacity increased. This phenomenon should be ascribed to the hollow nanosphere architecture of the as-prepared PPy materials, which induces electrolyte gradually infiltrates the electrode materials and increase the contact area between the electrode and electrolyte along with the cycling process.[22] Along with the cycle number increase, the charge transfer resistance of the testing cell was increased, from ~ 60 Ω cm^2 after 5 cycles to ~ 96 Ω cm^2 after 10 cycles, and maintained between 90 - 115 Ω cm^2 from 20 cycles to 50 cycles. After 50 cycles, it stabled at around 150 Ω cm^2, which is almost the same as fresh cell's charge transfer resistance, indicating the electrochemical stability of the as-prepared PPy hollow nanospheres. As reported previously, the increase in resistance of the PPy electrodes should be due to the intercalation mechanism.[23] When the diffusion length for the intercalating ions is increased, the charge transfer resistance will be increased, which was described as "shallow trapping" and "deep trapping".[24] Along with the increasing number of charge and discharge cycles, the swelling and/or decomposition of electrolyte will increase the penetrating distance of the sodium ions into the electrode. This increased distance shows a larger diffusion barrier for the sodium ions. Therefore, the sodium ions cannot diffuse at a sufficient rate, resulting into the increased resistances.

Furthermore, we measured cyclic voltammetry of the electrode before and after charge and discharge tests as shown in Fig. S6 (SI). It can be seen that the CV curves from fresh cell to the cell after 100 cycles demonstrated well-defined redox peaks with almost the same peak areas at ~ 2.4 and ~ 2.7 V during cathodic discharge and anodic charge processes, respectively. Furthermore, the CV curves almost overlapped over the 100 cycles, suggesting the as-prepared PPy hollow nanospheres can keep the constant cathodic discharge and anodic charge during the cycling.

To further understand the mechanism of sodium ion storage in the as-prepared PPy hollow nanospheres, *ex-situ* SEM, TEM, FTIR spectroscopy, and Raman spectroscopy were measured. We monitored the bond vibrations of the PPy hollow nanospheres before cycling and after 100 cycles (charged state), as shown in Fig. 3(a, b). In the Raman spectra (Fig. 3(a)), it can be observed that the Raman shift at 1555 cm^{-1} represents C=C symmetry stretching.[25-27] The two peaks located at 1405 and 1324 cm^{-1} can be assigned to the inter-ring (C–C) stretching.[28, 29] The vibrations at 1264, 1044, and 1033 cm^{-1} are attributed to a ring deformation mode.[26, 27] The bands with double peaks at 920 and 870 cm^{-1} are attributed to the C-H in-plane deformation.[30] The band at 686 cm^{-1} is assigned to ring deformation associated with the radical cation.[29, 31] After 100 cycles (charged state), the PPy hollow nanospheres exhibit almost the same Raman spectrum as that of the fresh electrode (shown in Fig. 3(a)), suggesting the stability of the as-prepared PPy hollow nanospheres after long cycles of doping / de-doping reactions.

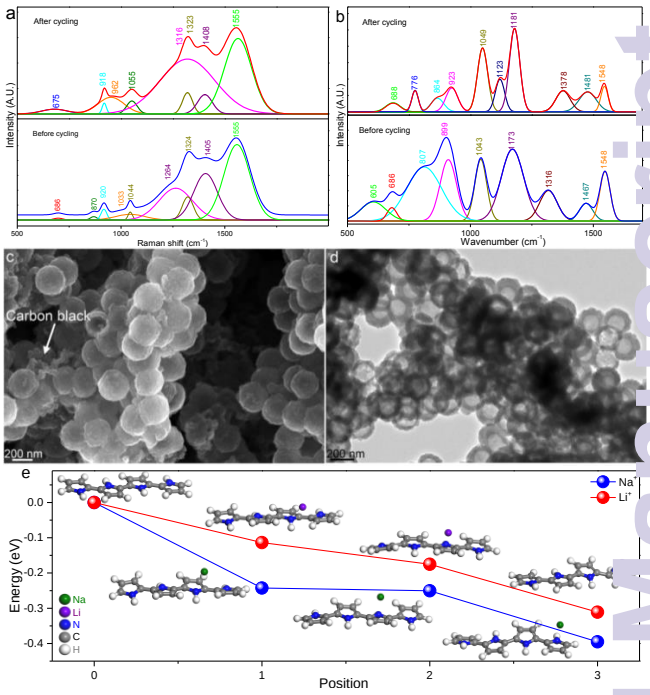

Fig. 3. (a) Raman scattering spectra of PPy hollow nanosphere electrode before cycling and after 100 cycles (charged state). (b) FTIR spectra of PPy hollow nanosphere electrodes before cycling and after 100 cycles (charged state). (c) FESEM image and (d) TEM image of PPy hollow nanosphere electrode after 100 cycles. (e) Enegy barriers of sodiated/lithiated PPy with Na/Li ion on different positions.

The stability of the PPy hollow nanoshperes was also confirmed by the FTIR spectra, as shown in Fig. 3(b). Before cycling, the FTIR spectrum of the PPy hollow nanospheres exhibited characteristic absorptions at 1548 cm^{-1}, which should be predominantlhy assigned to the C=C and C–C bonds in ring stretching mode. The peak at 1481 cm^{-1} predominantly comes from the C=C and C–N stretching mode. The bond vibration at 1316 cm^{-1} is derived from -C-N stretching, while the bond vibration at 1043 cm^{-1} should correspond to –C–H in-plane deformation. The peaks at 807, 686, and 606 cm^{-1} can be ascribed to C–H/N–H/C=C-C/C=C-N/C-N-C out-of-plane bending.[32, 33]

The characteristic bipolaron bands at 899 and 1173 cm^{-1} indicate that the PPy was in its doped state.[34] The discharge and charge process is mainly attributable to the reversible doping-de- doping mechanism of polypyrrole in the cathode.[34] During the discharge process, the doped polypyrrole is reduced, and the anions are stripped into the electrolyte, while the sodium ions act as counter ions to balance the charge. The anions would then be doped into the polypyrrole during the charge process, and it is expected to be highly reversible. Further experiments have confirmed this. When the PPy hollow nanosphere electrode was cycled 100 times, apart from a slight shift between the bond vibration positions, there is no obvious change, indicating that the PPy chains were preserved intact after chemical doping–de-doping. Furthermore, the morphology and the hollow nanosphere architecture were maintained after 100 cycles, as shown in the *ex-situ* SEM and TEM images (Fig. 3(c, d), respectively). The PPy hollow nanospheres were not filled with any products, which can be of benefit to the cyclablity of the electrode. To confirm the Na ion storage mechanism in the PPy cathode, we conducted density function theory (DFT) calculation on the energy barriers of sodiated PPy, as shown in Fig. 3e. Based on the experiment results, 4 unit PPy absorbed 1 Na ion ($[C_4H_5N]_4Na$), enegy barriers of sodiated PPy with Na ion on different positions were calculated. After the relax optimization, it can be seen that all possible

sodiated PPy positions, which are 1: on the bond between two [C_4H_5N] rings, 2: in the middle of the inside [C_4H_5N] ring, 3: in the middle of the outside [C_4H_5N] ring, are given the negative energy barriers (-0.24 eV for position 1, -0.25 eV for position 2, -0.40 eV for position 3). Therefore, the sodium ion absorption process is spontaneous behavior. The calculations confirm that the Na ion storage is the absorption process, which is consisted with the reported assumption on the Na ion storage in polymer cathode for Na-ion batteries.[16, 35] Furthermore, the most stable position for storage of Na ion locates in the outside [C_4H_5N] ring, because it achieves the lowest energy barrier. Surprisingly, we compared the storage of the Li ion in the same PPy positions, it was found that although the lithiated process is also spontaneous process due to the obtained negative energy barriers, the energy barrier values are higher than that of sodiated PPy (-0.11 eV for position 1, -0.18 eV for position 2, -0.31 eV for position 3), as shown in Fig. 3e. This indicates that PPy has better storage capability for Na ions than that of Li ions. Moreover, the experiment results confirm this theoretical calculation result that less than 50 mA h g^{-1} discharge capacity was obtained when the as-prepared PPy was worked as cathode material for Li-ion batteries (Fig. S7 (SI)).

The as-prepared PPy hollow nanospheres have demonstrated high current rate capacity and cyclability. Furthermore, because of the structural flexibility and stability of the redox-active polymers, the nanosphere electrode has superior stable rate capability. It was recently reported that a hollow sphere will endure ~ 5 times lower maximum tensile stress than that in a solid sphere with an equal volume during the lithiation process, which can provide better properties.[36-38] This can enhance the stable cyclability of the PPy hollow nanospheres as cathode materials in Na-ion batteries.

In summary, we have successfully prepared PPy hollow nanospheres as cathode materials for Na-ion batteries. Through *ex-situ* SEM, TEM, FTIR, Raman measurements and DFT calculation, it was revealed that the PPy hollow nanospheres function through reversible doping / de-doping reactions during the charge/discharge processes. PPy hollow spheres exhibited a specific capacity of 100 mA h g^{-1}, stable cyclability, and superior rate capability. The polymers can be prepared from low-cost and environmently benign organic sources. Therefore, Na-ion batteries with polymer electrodes could be developed for low cost energy storage and conversion.

Notes and references

[a] *Centre for Clean Energy Technology, Faculty of Science, University of Technology, Sydney, NSW 2007, Australia. Fax: +61-2-9514-1460; Tel: +61-2-9514-1741; E-mail: Dawei.Su@uts.edu.au, Guoxiu.Wang@uts.edu.au*

[b] *Institute for Superconducting and Electronic Materials, University of Wollongong, Wollongong, NSW 2522, Australia. Fax: +61-2-4221-5731; Tel: +61-2-4221-4558;*

[c] *College of Material Science and Technology, Nanjing University of Aeronautics and Astronautics, Nanjing, 210016 P.R. China*

† Electronic Supplementary Information (ESI) available: Detailed experimental procedures; FESEM, TEM images; Nitrogen sorption isotherm, Nyquist diagram and CV curves of the PPy hollow nanospheres electrode before and after different charge and discharge cycles and Cycling performance of PPy hollow nanospheres as cathode material for Li-ion battery. See DOI: 10.1039/b000000x/

ACKNOWLEDGMENT

This original research was proudly supported by the Commonwealth of Australia through the Automotive Australia 2020 Cooperative Research Centre (AutoCRC) and the Fundamental Research Funds for the Central Universities of China (NE2014301). The research used equipment located at the UOW Electron Microscopy Centre, which was funded by an Australian Research Council (ARC) Linkage, Infrastructure, Equipment and Facilities (LIEF) grant (LE0237478). The authors also would like to thank Dr. Tania Silver for critical reading.

1. S. W. Kim, D. H. Seo, X. Ma, G. Ceder and K. Kang, *Adv. Energy Mater.*, 2012, **2**, 710-721.
2. V. Palomares, P. Serras, I. Villaluenga, K. B. Hueso, J. Carretero González and T. Rojo, *Energy Environ. Sci.*, 2012, **5**, 5884-5901.
3. Y. Cao, L. Xiao, M. L. Sushko, W. Wang, B. Schwenzer, J. Xiao, Z. Nie, L. V. Saraf, Z. Yang and J. Liu, *Nano Lett.*, 2012, **12**, 3783-3787.
4. R. Berthelot, D. Carlier and C. Delmas, *Nat. Mater.*, 2011, **10**, 74.
5. M. M. Doeff, Y. P. Ma, M. Y. Peng, S. J. Visco and L. C. Dejonghe, *Energy Environment Economics: 28th Intersociety Energy Conversion Engineering Conference (Iecec-93), Vol 1*, 1993, 1111-1116.
6. Y. Zhu, Y. Xu, Y. Liu, C. Luo and C. Wang, *Nanoscale*, 2013, **5**, 780-787.
7. C.-Y. Chen, K. Matsumoto, T. Nohira, R. Hagiwara, Y. Orikasa and Y. Uchimoto, *J. Power Sources*, 2014, **246**, 783-787.
8. J. Goodenough, H.-P. Hong and J. Kafalas, *Mater. Res. Bull.*, 1976, **11**, 203-220.
9. I. D. Gocheva, M. Nishijima, T. Doi, S. Okada, J. Yamaki and T. Nishida, *J. Power Sources*, 2009, **187**, 247-252.
10. Y. Yamada, T. Doi, I. Tanaka, S. Okada and J. Yamaki, *J. Power Sources*, 2011, **196**, 4837-4841.
11. R. Tripathi, S. M. Wood, M. S. Islam and L. F. Nazar, *Energy Environ. Sci.*, 2013, **6**, 2257.
12. Y. Park, D. S. Shin, S. H. Woo, N. S. Choi, K. H. Shin, S. M. Oh, K. T. Lee and S. Y. Hong, *Adv. Mater.*, 2012, **24**, 3562-3567.
13. W. Deng, X. Liang, X. Wu, J. Qian, Y. Cao, X. Ai, J. Feng and H. Yang, *Sci Rep*, 2013, **3**, 2671.
14. L. Zhao, J. Zhao, Y. S. Hu, H. Li, Z. Zhou, M. Armand and L. Chen, *Adv. Energy Mater.*, 2012, **2**, 962-965.
15. R. Zhao, L. Zhu, Y. Cao, X. Ai and H. X. Yang, *Electrochem. Commun.*, 2012, **21**, 36-38.
16. L. Zhu, Y. Shen, M. Sun, J. Qian, Y. Cao, X. Ai and H. Yang, *Chem. Commun.*, 2013, **49**, 11370-11372.
17. L. Zhu, Y. Niu, Y. Cao, A. Lei, X. Ai and H. Yang, *Electrochim. Acta*, 2012, **78**, 27-31.
18. J.-J. Ding, Y.-N. Zhou, Q. Sun and Z.-W. Fu, *Electrochem. Commun.*, 2012, **22**, 85-88.
19. J. J. Ding, Y. N. Zhou, Q. Sun, X. Q. Yu, X. Q. Yang and Z. W. Fu, *Electrochim. Acta*, 2013, **87**, 388-393.
20. S. Komaba, N. Yabuuchi, T. Nakayama, A. Ogata, T. Ishikawa and I. Nakai, *Inorg. Chem.*, 2012, **51**, 6211-6220.
21. M. Sathiya, K. Hemalatha, K. Ramesha, J. M. Tarascon and A. S. Prakash, *Chem. Mater.*, 2012, **24**, 1846-1853.
22. L. Yu, L. Zhang, H. B. Wu and X. W. Lou, *Angewandte Chemie*, 2014, **126**, 3785-3788.
23. J. Killian, B. Coffey, F. Gao, T. Poehler and P. Searson, *J. Electrochem. Soc.*, 1996, **143**, 936-942.
24. J. Tanguy, N. Mermilliod and M. Hoclet, *J. Electrochem. Soc.*, 1987, **134**, 795-802.
25. Y.-C. Liu and B.-J. Hwang, *Synthetic Met.*, 2000, **113**, 203-207.
26. A. B. Gonçalves, A. S. Mangrich and A. J. G. Zarbin, *Synthetic Met.*, 2000, **114**, 119-124.
27. M. Grzeszczuk, A. Kępas, C. Kvarnstrom and A. Ivaska, *Synthetic Met.*, 2010, **160**, 636-642.
28. K. Crowley and J. Cassidy, *J. Electroanalytical Chem.*, 2003, **547**, 75-82.
29. M. Santos, A. Brolo and E. Girotto, *Electrochim. Acta*, 2007, **52**, 6141-6145.
30. Y.-C. Liu, B.-J. Hwang, W.-J. Jian and R. Santhanam, *Thin Solid Films*, 2000, **374**, 85-91.
31. K. Crowley and J. Cassidy, *J. Electroanal. Chem.*, 2003, **547**, 75-82.
32. S. Ye, L. Fang and Y. Lu, *Phys. Chem. Chem. Phys.*, 2009, **11**, 2480-2484.
33. R. Kostić, D. Raković, S. A. Stepanyan, I. E. Davidova and L. A. Gribov, *J. Chem. Phys.*, 1995, **102**, 3104-3109.
34. Y. Lu, G. Shi, C. Li and Y. Liang, *J. appl. polymer sci.*, 1998, **70**, 2169-2172.
35. M. Zhou, Y. Xiong, Y. Cao, X. Ai and H. Yang, *J. Polym. Sci. Pol. Phys.*, 2013, **51**, 114-118.
36. Y. Yao, M. T. McDowell, I. Ryu, H. Wu, N. Liu, L. Hu, W. D. Nix and Y. Cui, *Nano Lett.*, 2011, **11**, 2949-2954.
37. X. Lai, J. Li, B. A. Korgel, Z. Dong, Z. Li, F. Su, J. Du and D. Wang, *Angew. Chem. In. Edit.*, 2011, **50**, 2738-2741.
38. Z. Li, X. Lai, H. Wang, D. Mao, C. Xing and D. Wang, *J. Phys. Chem. C*, 2009, **113**, 2792-2797.